Potential of the Bucharest 3 MV Tandetron™ for IBA Studies of Deer Antler Mineralization

S. Gomez[1], A. Garcia[2], T. Landete-Castillejos[2], D. Pantelica[3], Ana Pantelica[3], E.A. Preoteasa[3], Adela Scafes[3], M. Straticiuc[3]

[1]Departamento Anatomía Patológica, University of Cadiz, Spain
[2]IREC, Sección Albacete (CSIC-UCLM-JCCM), University of Castilla-La Mancha, Albacete, Spain
[3]Horia Hulubei National Institute for Physics and Nuclear Engineering, Bucharest-Magurele, Romania

Con formato: Español (alfab. internacional)

Abstract

Combined PIXE and PIGE analysis was applied at the new Bucharest Tandetron to investigate biomineralization in two calcified tissues, deer antlers and femur bone. By annual loss and fast re-growth, antlers are a valuable model for bone as a dynamical system. Samples characterized by optical microscopy and histology were analyzed for P, Ca, F, Na, Mg, S, Cl, K, Zn, Sr by 3 MeV proton simultaneous PIXE and PIGE, using a hydroxyapatite standard and other reference materials. Good correlation between methods was found for P, and the concentrations were related to biological data. Antlers showed lower mineralization than femur, with the lowest values in the third antler beam. A power function of mineralization vs. “mineral age” of antlers was found. Thus combined PIXE and PIGE of antlers may bring highly relevant insights in biomineralization research.

PACS:
Keywords: Bone, antler, PIXE, PIGE, tandem accelerator

Introduction

A new 3 MV tandem accelerator for applications of Ion Beam Analysis (IBA) has been commissioned at the Horia Hulubei Nuclear Institute for Physics and Nuclear Engineering (NIPNE-HH) at Bucharest, and it is already in use for diagnosis and characterization of a wide variety of special materials. The present study is intended for the evaluation of this machine’s potential for biological applications. To this purpose, we approached a comparative analysis of the mineral composition of deer antlers and bones, a type of calcified tissue that has not been studied before by IBA techniques.

Antlers are bony cranial appendages of the deer characterized by an annual cycle of loss and re-growth. They are the fastest growing bones in mammals, which makes them a valuable model for studying mineralization of primary bone and the influence of hormonal, dietary and pollution factors. Antlers are typically formed in 120-150 days, but their cortical bone is formed beginning on the 70th day of growth. A time-resolved view on mineralization status can be obtained by taking samples from the first, second and third antler beam and labeling with calcein, a fluorescent indicator for bone formation. Our group performed detailed studies of antlers by other methods [1-2].

The IBA experimental set-up at the 3 MV Tandetron of NIPNE-HH permits to concomitantly register PIXE, PIGE and RBS spectra using specific HPGe Ortec detectors. The simultaneous detection of PIXE, PIGE and RBS spectra gives

complementary information (a “total IBA” approach [3]).
Experimental and theoretical aspects as well as general applications of these methods have been treated together in studies of techniques intercomparison and intercalibration standards [4-10]
The combined IBA approach was applied by other groups to bones [11],dental enamel [12-13],and rough hydroxyapatite [14]. Previously our group used IBA methods to the study of bones [15],dental enamel [16], dental composites [17, 18],and other biological materials [19-21].One major difficulty of IBA on biomineral structures is that, generally, they are thick and granular samples and, implicitly, the PIXE and PIGE spectra are affected by matrix effects. However, quantitative analysis of thick calcified tissue samples such as antlers and bones could be done by using thick samples of reference materials. In the preliminary approach of the present study we will limit ourselves to PIXE and PIGE analysis of antlers and femur bone. The applications of RBS to this type of biomineral structures will make the object of further developments.

Materials and Methods

Biological samples taking-off

Hard antlers were obtained from three Iberian red deer stags selected from a herd kept at an experimental farm at the University of Castilla-La Mancha (Spain). During the growing period of the antler deers received one injection of calcein, a fluorescent indicator (5mg/Kg body wt) on the 117th day in order to label the bone formation. Hard antlers were sawn off according to farm protocols. Because antlers are dead when they are hard and clean of velvet, antler removal produces no pain and no anesthesia is required. Nevertheless, a low dose of xylazine (0.3 mg/kg body wt) was used as tranquilizer to minimize suffering. One centimeter thick slices were cut at 3 levels from the labeled antlers: in the first third of the main beam above the bez tine (Pos 1), in the second third below the crown (Pos 2), and in the middle of third (Pos 3) (Fig.1a). Other bone samples were femur from yearling deer and adult deer. Femurs were processed in the same way as antler.

Optical microscopy and histology

For histological analysis, dehydrated portions of the slices were embedded in poly-methyl-methacrylate (PMMA). Mineralized ground sections (50µm-thick) were prepared by the sawing–polishing method described previously [1-2]. Sections were first examined with episcopic-fluorescence microscopy using a Nikon Optiphot 2 EFD-3 (Tokyo, Japan) microscope to identify the calcein labels in primary osteons (Fig.1b). Then sections were stained with von Kossa for microstructure. Label distances within a single osteon as well as osteon diameters were measured using Image J program (NIH, USA), and the elapsed time since the osteon formation to velvet shedding (on the 150th day) was calculated for each position considering a mineral apposition rate (thickness of the layer created and mineralized in one day onto a bone surface) of 2µm/day [2].This estimated time was considered as the 'mineral age', and used as a reference time to reconstruct the proximodistal mineralization sequence in the antler.

Preparation of samples for IBA invetsigation

Mineralized thin sections (100 µm-thick) of the antlers and femur bone were prepared and glued with cyanoacrylate onto a carbon (high-purity graphite) planchet (nº76270 EMS). A few other sections were 1 mm thick. Concentrations are reported to dry tissue.

The Bucharest 3 MV Tandetron™

The Bucharest 3 MV Tandetron™(High Voltage Engineering Europe B.V., Amersfoort, Netherlands) is a last-generation integrated instrument for IBA and ion implantation. It is provided with Cockroft-Walton power supply and, in the actual IBA configuration PIXE, PIGE and RBS spectra are recorded simultaneously, with automatic control and recording of measurement parameters.
Target viewing with an optical system and XYZ/goniometric positioning of specimen allows a precise selection of the analyzed area. The size of the beam spot can be focused between 2 mm and 20 µm. These two features represent a major advantage for studies of heterogeneous biological samples.
For PIXE, an IGLET X-series detector (with a 12.7 µm thick Be window, energy range 1.5 keV – 1 MeV without Be window) with energy resolution of 140 eV at 5.9 keV (55Fe), was mounted inside the reaction chamber.
For PIGE, a GEM10P4-70 gamma-ray detector (energy range 40 keV – 10 MeV) with energy resolution of 1.75 keV at 1.33 MeV (^{60}Co) was situated at about 15 cm from the target, outside of the reaction chamber.
For RBS, two ion-implanted silicon detectors for charged particle are available, one fixed and one movable, with a 16 keV energy resolution for a 2 MeV He beam.

Particle beam, target characteristics and irradiation damage

The targets were positioned normal on the beam direction. PIXE and PIGE detectors were placed at 45° with respect to the beam.
A 3 MeV proton beam was used and PIXE and PIGE spectra were simultaneously detected (Fig. 1 c,d). Beam was defocused (ϕ = 1-2 mm) and beam current was in the range of 1-7 nA to limit sample damage, but this could not be completely prevented. A dark coloration was produced, and the spot was clearly contrasted in fluorescence microscopy (Fig. 1e). It could be due to charring of the organic component of the mineralized tissue, but also to the generation of color centers (F centers) [22] in hydroxyapatite. This is suggested by the dark spot formation on pure KCl pellets used as standards. Whether the coloration was associated or not with significant changes of some elements' concentrations remains to be investigated in future work. Exposure time was of 15-90 min, and collected electrical charge was of 1-25 µC. The collected charge was measured using a current digitizer. No electron suppression was used. Although this method is rather approximate with thick electroinsulating targets as ours, it may serve for a sufficiently accurate normalization of the spectra by making use of the collected charge for thick pellets of reference materials.

Reference materials

Certified reference materials (CRMs) used as standards and/or for analytical quality control included pelleted hydroxyapatite (bone ash) (NIST SRM-1400), fluorspar (NIST SRM-180), glass (NIST-611), soil (SS-P, Kosice, SK), and IAEA-V-10 (hay). In addition, pellets of high purity chemical compounds (KCl, NaCl, Fe2P, S, CaSO4, CaCO3, CaF2, LiF, and MgO) were used for PIXE calibration and/or quantitative standardization for PIGE.

PIXE measuremets

The PIXE experiments were performed both without filter and with an Al filter of 20 µm thickness, in view of reducing the high intensity low energy energy $K_{\alpha}$and K_{β} X-ray peaks of major elements P and Ca, and thus to improve the analytical sensitivity for higher Z elements (lower pile-up effects). Spectra without filter were collected for 15 min in view of analyzing P and Ca and some biologically important minor elements (S, Cl, K). Spectra with Al filter were collected for 45 – 90 min for the analysis of trace elements, in particular Zn and Sr. The detector-target distance was of ~ 24 cm in the case of PIXE without filter and of ~12 cm for PIXE with Al filter. The detection dead time was lower than 10-12 %.
For a quantitative analysis the PIXE spectra were processed by thick-target GUPIX program calculations [23]. In addition, a relative standardization method based on reference materials was used. The spectra were processed by background subtraction and Gaussian least square fit of lines using Leone (a modified version of a program for multi-peak spectra by H. Hanewinkel, Institute for Nuclear Physics of Koln, Germany) and the GammaW program ( ).
The detection limits estimated with GUPIX for Zn and Sr were of about ~ 50 µg/g for Zn and ~100 µg/g for Sr in measurements without filter and of ~25 µg/g and ~50 µg/g, respectively, when the 20 µm Al filter was used. These values were well below the reference values in the hydroxyapatite standard and the estimated concentrations in antlers and femur bone.

PIGE measurements

The following PIGE reactions were considered (Table 1).
Attention was paid to the PIGE interference reactions in producing ^{24}Mg and ^{28}Si (experimental correction factors in parentheses): ^{27}Al(p,$\alpha\gamma$)^{24}Mg ($A_{1014.4\ keV}/A_{1368.6\ keV}$ = 15.0 ± 1.4%); ^{31}P(p, $\alpha\gamma$)^{28}Si ($A_{1266.1\ keV}/A_{1779\ keV}$ = 50.3 ± 5.8%); ^{27}Al(p,γ)^{28}Si ($A_{1014.4\ keV}/A_{1779\ keV}$ = 382 ± 5.8%). In addition, a spectral interference between ^{25}Mg (585 keV) and the natural background line of 583 keV (^{208}Tl) has been considered.

For PIGE standardization, a relative analytical method was applied with standards of certified element concentration, using the following formula [24]:

$$c_T = (Y_T \cdot S_{T(E1/2)} / Y_S \cdot S_{S(E1/2)}) \cdot c_S \quad (1)$$

where c_T and c_S , are the element concentrations (mass fractions) in sample and standard, respectively; Y_T and Y_S , are element gamma-ray yields for sample and standard, respectively, normalized to the beam charge of the incident protons; S_T and S_S , are stopping powers for proton beam of energy

$E_{1/2}$. To assess the stopping power values for various matrices (bone, chemical compounds as comparator standards, as well as NIST and IAEA CRMs) the SRIM simulation program was used [25].

To assess the proton beam energy $E_{1/2}$, defined as $Y(E_{1/2}) = Y(E_p) / 2$), we measured excitation functions using proton beam energies between 2.4 and 3 MeV (energy step of 0.1 MeV) both for antler samples and standards.

Results and Discussions

In the PIXE spectra up to 17 elements could be detected when processed with GUPIX, but of those we focused for quantitative analysis only on the major elements (P, Ca) and on a few minor and trace elements of higher biological relevance (S, Cl, K, Sr, Zn).

Although Al was also evidenced by PIXE when using the Al filter and by PIGE, it was ignored because probably it was not genuine (X-ray fluorescence from the filter; possible contaminant).

The major elements in the analyzed antler and femur samples (Table 2) are constituents of hydroxyapatite (HA), the main mineral in most calcified tissues. However, in biomineral structures HA is associated with other Ca compounds, and the [Ca]/[P] ratio is a relevant indicator of the mineral composition. For pure hydroxyapatite, $Ca_{10}(PO4)_6(OH)_2$, the ratio is 2.157; for our bone ash reference material it is slightly lower, 2.132. In femur samples the [Ca]/[P] ratio showed the closest values (2.27 – 2.32) to that of the bone ash HA standard, as one could expect based on their similar origin. In all types of analyzed biomineral samples and especially in antlers, the [Ca]/[P] ratio was higher than in HA, suggesting the possible presence of fractions of Ca compounds with relative lower P and/or higher Ca content (e.g., calcium carbonate, $CaCO_3$; β-tricalcium phosphate) together with HA. However, while the concentrations of P and Ca were much lower in antlers as compared to the bone ash standard, the [Ca]/[P] ratio values did not show appreciable differences, thus HA was the main inorganic compound of antlers. As compared to femur (from yearling and adult deer), antlers showed lower Ca and P as well as a higher [Ca]/[P] ratio of 2.34 – 2.46, indicating thus a significantly lower degree of mineralization with respect to the bone. The lowest values of Ca and P as well as the highest value of the [Ca]/[P] ratio were found in the 3rd beam of antlers, in contrast to the 2nd and 1st beams. The order of Ca and P concentrations in the three antler beams was 1st≥ 2nd > 3rd. This illustrates the fact that the mineralization process was completed in the 2nd and 1st antler beams but was unfinished in the 3rd beam, in agreement with the present optical microscopy results (Fig. 1b) and with previous data by other methods [1]. Also this explains why antlers break most frequently at the 3rd beam. Finally the data of 1st antler beam show large

241 statistical spread of Ca and P, due to appreciable differences between antlers
242 from different animals.

243 Most interesting, if the mineralization degree of antlers – defined by the
244 position-dependent relative Ca concentration in antlers with respect to pure HA
245 or to bone ash HA standard – is represented as a function of the time moment
246 when the antler was mineralized, the data points can be fitted with the power
247 (Freundlich) function (Fig. 2):

248 $$[Ca]/[Ca]_{max} = at^{\beta},\ 0 < \beta < 1 \qquad (2)$$

249 This function is the solution of the simple differential equation:

250 $$d[Ca]/dt = \beta\,[Ca]/t \qquad (3)$$

251 which evidences a single and unitary mechanism of mineralization, probably
252 based on HA microcrystal growth in the calcified tissue, throughout the whole
253 investigated time domain (one year). This remarkable analytical law of the
254 mineralization process is at variance with the current empirical view which
255 arbitrarily distinguishes a fast initial phase of growth up to 70 %, followed by a
256 further slow phase, each one with its own mechanism.

257 The PIGE analysis detected the minor elements F, Na,P and Mg (Table 3). P
258 was detected both by PIGE and PIXE, and Fig. 3 shows an excellent linear
259 correlation ($p < 0{,}000001$) between the values of [P] analyzed by the two
260 methods. For instance, P level was higher in femur than in antlers by both
261 techniques. Na and Mg were also higher in the bone, while F was appreciably
262 higher in antlers. It is plausible that Mg^{2+} could substitute Ca^{2+} in HA from the
263 calcified tissues; in fact HA content was higher in femur than in antlers as
264 shown by higher P and Ca. On the other hand, monovalent ions like F^- and Na^+
265 could bind electrostatically to ionic groups, both in antlers and in femur.

266 Comparing the concentrations in the antler's three beams, the order ($1^{st} \gtrsim 2^{nd} >$
267 3^{rd}) was found for Na and for F. This seems to be consistent with a lower
268 mineralization in the 3^{rd} beam and with the electrostatic (weak) adsorption of F^-
269 and Na^+ on ionic sites from the inorganic phase (HA crystallites) rather than
270 from proteins. Alternatively, F^- may substitute OH^- ions in HA, forming
271 fluoroapatite. Neither hypothesis does explain why F^- was lower in adult bone
272 as compared to antlers. Thus binding mechanisms of F^- (and Na^+) in antlers
273 and bone still remain unclear.

274 The following biologically important minor and trace elements – S, Cl, K, Zn, Sr
275 - were detected by PIXE:. While the concentrations of K, Zn, Sr in antlers and
276 femur could be evaluated by comparison with the HA (bone ash) reference
277 material, S and Cl were not present in the HA standard. Therefore we had the
278 following options: 1) to extrapolate for these elements the yield vs. Z curve

obtained for the standard (Fig.4), and 2) to use additional reference materials like CaSO4, pure metaloid S, KCl, NaCl. The results are presented in Table 4.

Sulfur was assigned mainly to sulphated glycans from the organic fraction of antlers, as sustained by its lowest concentration in femur, intermediate values in 1st and 2nd antler beams, and highest level in 3rd antler beam. This corresponds to an increasing scale of organic content and biochemical activity (lowest in femur and highest in 3rd antler beam). Cl and K followed parallel trends having higher values in antlers as compared to femur. Sr, a chemical analogue of Ca, was also higher in antlers than in femur, a trend contrary to Ca. This suggests that probably Sr substituted Ca in HA only when Ca was not in excess. Finally Zn, which plays an essential role for biomineralization as constituent of the active site of the alkaline phosphatase enzyme, but which is bound also as a passive metallic ion in other sites of normal compact bone [15],showed an irregular distribution in antlers and femur. We noted that Zn was lower in the 3rd antler beam of a case where osteomalacia (softening caused by defective mineralization) occurred [1]. Nevertheless, the incertitudes in the analysis of Sr and Zn traces were high and more precise determinations are needed.

Conclusions

The combined PIXE and PIGE analysis of deer antlers and femur yielded biologically relevant results. This approach allowed a precise survey of the biomineralization status of the bone and of the main three beams of antlers by time-resolved monitoring of P and Ca, as well as of compositional differences revealed by the Ca/P ratio. Significant differences between antlers from different animals were found. The 3rd antler beam appeared less mineralized as compared to 2nd and 1st antler beams, in agreement with optical microscopy results and data obtained by other methods. At the same time a general evolution law (power function) of mineralization has been found, consistent with a unique mechanism of biomineralization. A very good linear correlation between PIXE and PIGE measurements of P has been evidenced. Minor elements like F, Na,Mg, Al, S, Cl, and K detected by both methods reveal secondary interactions in the calcified tissues. The analysis of trace elements Sr and Zn was still imprecise, but further experimental improvements are the object of our future work. In brief, the simmultaneous PIXE and PIGE analysis provided a relevant insight of biomineralization in antlers and bones.

The main advantages of the 3 MV Tandetron for studies of antlers and other calcified tissues appeared to be the visualization of sample's surface and the precise positioning of the proton beam, the PIXE detection of biologically relevant light elements and the simultaneous detection of PIXE and PIGE

spectra (extension to RBS will be the object of future work). From the IBA perspective, the main disadvantages of biomineral structures are their electroinsulating character, strong matrix effects (thick samples), and heterogeneous structure, but these aspects are compensated by the advantage of the calcified tissues' physical-chemical stability. Thus the 3 MV Tandetron evidenced a high potential for studies of bone mineral and of antlers as a model system for biomineralization.

References

1. T. Landete-Castillejos, J.D. Currey, F. Ceacero, A.J. García, L. Gallego, S. Gomez, *Bone* **50** (2012) 245-254.
2. S. Gomez, A.J. Garcia, S. Luna, U. Kierdorf, H. Kierdorf, L. Gallego, T. Landete-Castillejos, *Bone* **52** (2013) 506-515,.
3. C. Jeynes, M.J. Bailey, N.J. Bright, M.E. Christopher, G.W. Grime, B.N. Jones, V.V. Palitsin, R.P. Webb, *Nucl. Instrum. Methods* B **271** (2012) 107-118.
4. IAEA, *Instrumentation for PIXE and RBS, IAEA-TECDOC-1190*, International Atomic Energy Agency, Vienna (2000).
5. A. Denker, W. Bohne, J. Rauschenberg, J. Röhrich; E. Strub, *CAS – CERN Accelerator School and KVI: Specialised CAS Course on Small Accelerators*, Zeegse, The Netherlands (2005) 417-432.
6. G. Demortier, *Nucl. Instrum. Methods* B **66** (1992) 51-64.
7. G. Demortier, *J. Electron Spectrosc. Rel. Phenom*. **129** (2003) 243–271.
8. I. Gomez-Morilla, A. Simon, R. Simon, Á.Z. Kiss, G.W. Grime, *Nucl. Instrum. Methods B* **249** (2006) 897-902.
9. U. Watjen, P. Maier-Komor, R. Pengo, N.J. Zaika, M. Budnar, V. Valkovic, *Nucl. Instrum. Methods* B **99** (1995) 376-379
10. U. Watjen, H. Bax, J. Raisanen, *Nucl. Instrum. Methods* B **118** (1996) 676-680.
11. C. Santos, M. Fonseca, V. Corregidor, H. Silva, H. Luís, A.P. Jesus, J. Branco, L.C. Alves, *Nucl. Instrum. Methods* B **331** (2014) 266–270
12. G. Demortier, S. Nammour, *Nucl. Instrum. Methods* B **266** (2008) 2408–2411.
13. C. Oprea, P.J. Szalanski, M.V. Gustova, I.A. Oprea, V. Buzguta, *Appl. Radiat. Isotopes* **67** (2009) 2142–2145
14. M.J. Bailey, S. Coe, D.M. Grant, G.W. Grime, C. Jeynes, *X-Ray Spectrom.*, *38* (2009) 343–347
15. S. Gomez, E.A. Preoteasa, L. Harangus, A. Iordan, D. Grambole, F. Herrmann, *Nucl. Instrum. Methods* B **249** (2006) 673-676,.
16. E.A. Preoteasa, Elena Preoteasa, A. Kuczumow, D. Gurban, D. Grambole, F. Herrmann. *X-ray Spectrom.* **37** (2008) 517-535.
17. E.A. Preoteasa, Elena S. Preoteasa, C. Ciortea, D.D. Marin, D. Gurban, M. Gugiu, Adela Scafes, *X-Ray Spectrom*. **38** (2009) 548-556.
18. Eugen A. Preoteasa, Elena S. Preoteasa, Ioana Suciu, *Atomic and Nuclear Surface Analysis Methods: A Novel Perspective for the Characterization of Dental Composites*, Nova Science Publishers, Inc., NY, 2012.
19. E.A. Preoteasa, M. Salagean, A. Pantelica, D. Plostinaru, B. Constantinescu, St. Berceanu, J. Radioanal. Nucl. Chem. Articles **151** (1991) 261
20. A. Pantelica, A. Ene, M. Gugiu, C. Ciortea, O. Constantinescu, Rom. Rep. Phys. **63** (2011) 997.
21. A. Pantelică, D. G. Ghita, D. Păceşilă, P. Ionescu, A. Scarlat, M. Drăguşin, *IBWAP-2014 Conference*, Constanta, Romania (2-7 July 2014).
22. C. Kittel, *Introduction to Solid State Physics. 4th Edition*, John Wiley & Sons, Inc., New York – London (1971).
23. J.L.Campbell, D. Higuchi, J.A. Maxwell, W.J. Teesdale, *Nucl. Instrum. Methods* **B 77** (1993) 95.
24. A. Savidou, X. Aslanoglou, T. Paradellis, M. Pilakouta, *Nucl. Instrum. Methods* B, **152** (1999) 12
25. J.F. Ziegler, *The Stopping and Range of Ions in Matter,* volumes 2 - 6, Pergamon Press, 1977-1985; J.F. Ziegler, *Nucl. Instrum. Methods* B, **219** (2004) 1027,

Con formato: Español (alfab. internacional)

Con formato: Español (alfab. internacional)

Con formato: Español (alfab. internacional)

Con formato: Español (alfab. internacional)

Con formato: Español (alfab. internacional)

Con formato: Español (alfab. internacional)

Con formato: Español (alfab. internacional)

Table 1. Nuclear reactions used in the PIGE analysis of calcified tissues and energies of their gamma radiations

Nuclear reaction	E_γ, keV
$^{19}F(p,p'\gamma)^{19}F$	109.9; 197.1 keV);
$^{23}Na(p,p'\gamma)^{23}Na$	(E_γ =440; 1636.0 keV),
$^{23}Na(p,\alpha\gamma)^{20}Ne$	(1633.6 keV);
$^{24}Mg(p,p'\gamma)^{24}Mg$	(1368.6 keV),
$^{25}Mg(p,p'\gamma)^{25}Mg$	(585 keV);
$^{31}P(p,p'\gamma)^{31}P$	(1266.1 keV);

Table 2. Major elements analyzed by PIXE and their ratio in samples of deer antlers and femur bone.

Calcified tissue	**[P]**	**[Ca]**	**[Ca]/[P]**
HA3Bone Ash standard	17.91 ± 0.19	38.18 ± 0.13	2,132 ± 0,024
Antler Pos. 3	8.57 ± 0.31	21.09 ± 0.77	2.463 ± 0.001
Antler Pos. 2	10.03 ± 0.89	23.8 ± 1.6	2.380 ± 0.049
Antler Pos. 1	11.7 ± 1.8	27.6 ± 4.1	2.367 ± 0.067
Femur, Yearling*	12.97 ± 0.25	29.59 ± 0.14	2.281 ± 0.030
Femur, Adult*	16.66 ± 0.28	39.79 ± 0.17	2.388 ± 0.034

*Single cases. Incertitudes are due only to PIXE measurements (no account of biological variability).

Table 3. Minor elements analyzed by PIGE in samples of deer antlers and femur bone.

Sample	**F (μg/g)**	**Na (%)**	**Mg (%)**	**P (%)**	**S_{sample} [keV/(mg/cm^2]**
Antler 3rd	**366**	**0.404**	< 0.38	**6.66**	109.5
Antler 2nd	**572**	**0.663**	< 0.38	**11.15**	106.3
Antler 1st	**649**	**0.781**	< 0.35	**11.13**	101.83
Femur, yearling	**549**	0.704		14.36	99.7
Femur, adult	**< 102**	**2.22**		**15.22**	99.7
s (%)	3-15	2-7	11-30	4-13	
Standard	Fluorspar NIST SRM-180 (CaF2, 98.8%)	NaCl	Hay IAEA-V10	Bone Ash NIST SRM-1400	
$S_{standard}$ [keV/(mg/cm^2]	86.13	83.25		86.23	

Table 4. Minor and trace elements detected by PIXE in samples of deer antlers and femur bone.

Table PIXE (Ep=3 MeV,)

Sample	S (ppm)	Cl (ppm)	K (ppm)	Sr (ppm)	Zn (ppm)	S [keV/ (mg/cm2]
Bone Ash NIST SRM-1400 Standard						
Antler 3rd	**1399**	**1580**	**1710**	**403**	**46.0**	109.5
Antler 2nd	**890**	**2530**	**2990**	**547**	**86.8**	106.3
Antler 1st	**859**	**1530**	**1170**	**570**	**84.8**	101.83
Femur, yearling				**595.5**	**70.8**	99.7
Femur, adult						99.7
σ (%)	**14–26**	**3–12**	**9–22**	15-17	8-14	
Bone Ash NIST SRM-1400 Standard				**249±7**	**181±3**	86.23

LEGEND OF FIGURES

Figure 1- Composition showing the analyzed positions of the antler (a), the calcein labeled antler sections and the microstructure of the antler at position 1,2, and 3 (c), a PIGE-spectra (d), and the beam impact area on the section surface as viewed with fluorescence microscopy (e).

Figure 2. - Percent mineral (Ca) content in deer antlers as measured by PIXE vs. elapsed time since the osteon formation. The data points were fitted with a power (Freundlich) function.

Figure 3. – Linear regression of the P concentrations measured by PIGE vs. PIXE in hydroxyapatite (bone ash standard). Assuming a bivariate normal distribution, the 95% confidence ellipses for the population mean (inner dash line) and for prediction (outer dash line) are shown, as well as the 95% confidence limits for PIGE (dot lines). The intercept close to 1 shows a linear correlation with good significance between the two methods ($p < 0.000001$).

Figure 4. – Plot of X-ray yield values in hydroxyapatite (bone ash standard) vs. Z, used for interpolating and extrapolating yield values, of particular interest for S and Cl. The experimental data points (black squares) and the inter/extrapolated points (open circles) are shown.

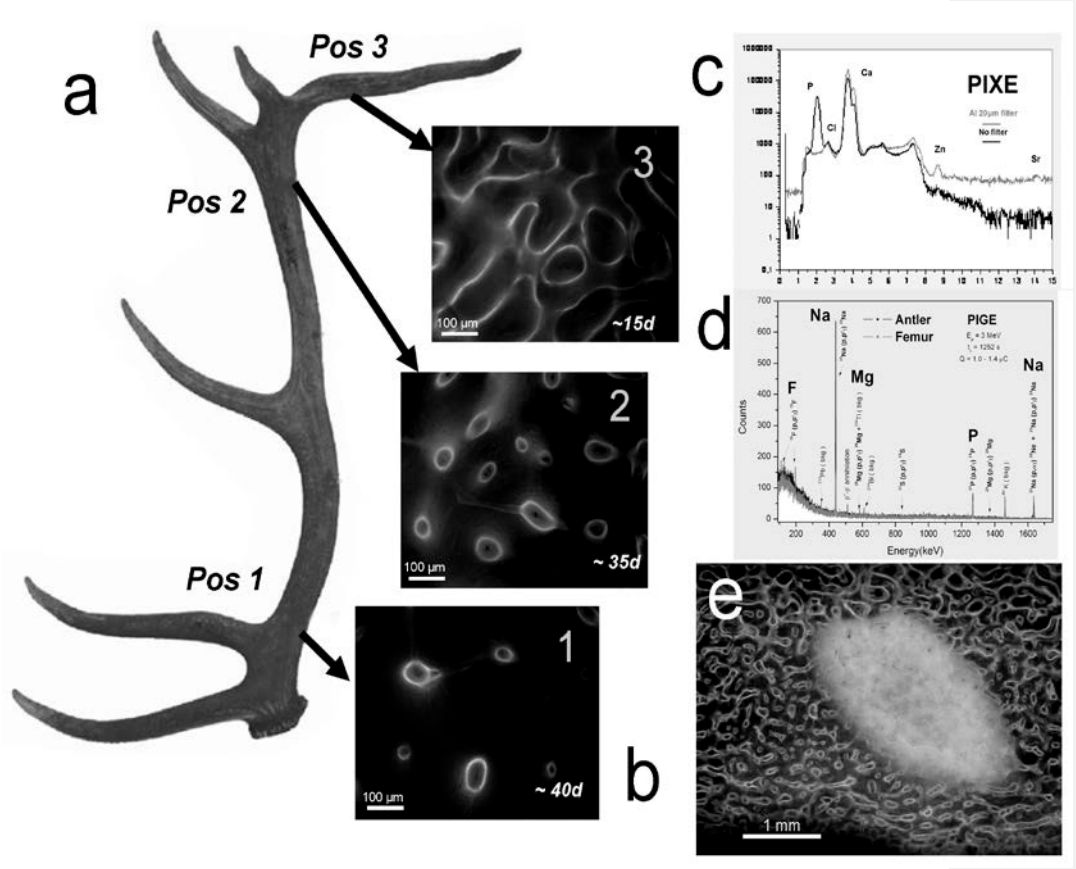
a
Pos 3
Pos 2
Pos 1
3
~15d
100 µm
2
~ 35d
100 µm
1
~ 40d
100 µm
b
c
PIXE
P
Cl
Ca
Zn
Sr
No filter
d
Na
Antler
Femur
PIGE
F
Mg
Na
P
Counts
Energy(keV)
e
1 mm

Figure 1

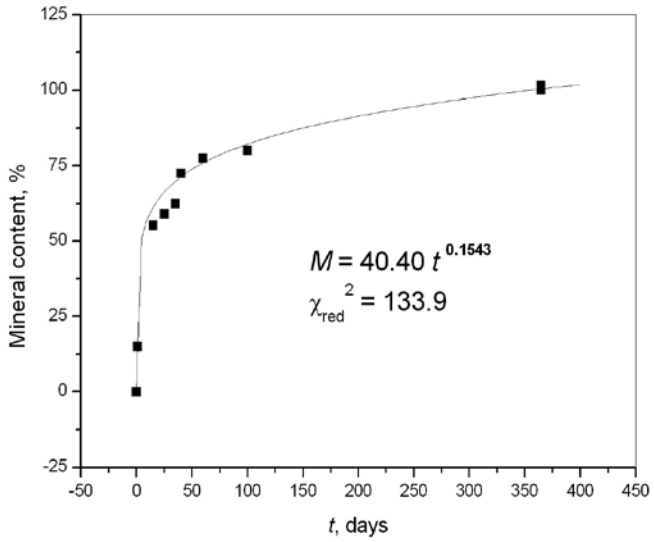

Figure 2

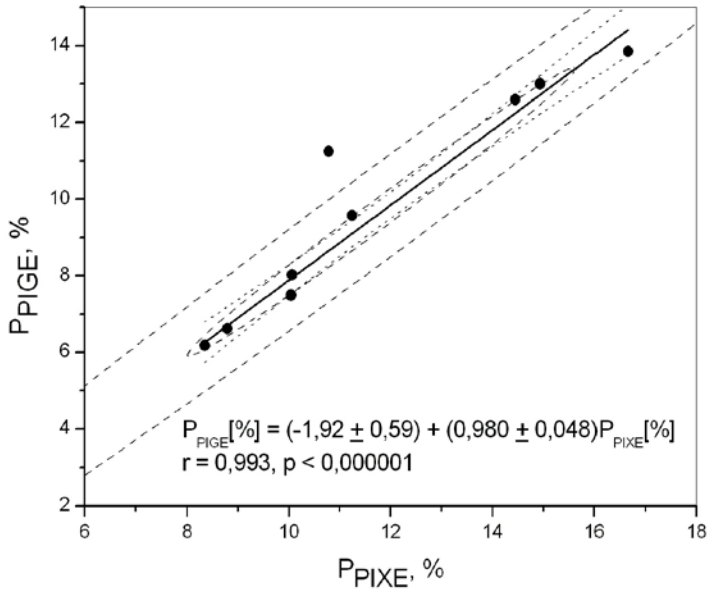

Figure 3

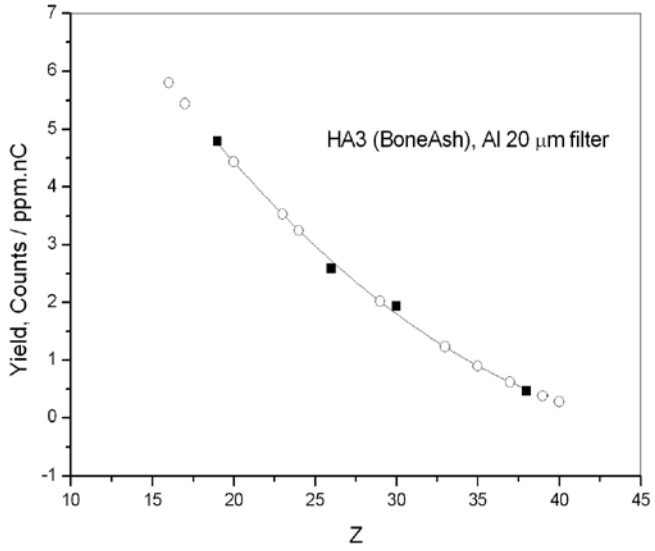
HA3 (BoneAsh), Al 20 μm filter
Yield, Counts / ppm.nC
Z
7
6
5
4
3
2
1
0
-1
10
15
20
25
30
35
40
45

Figure 4